Electronic Supplementary Information

Machine learning-aided unraveling of the importance of structural features for the electrocatalytic oxygen evolution reaction on multimetal oxides based on their A-site metal configurations

Yuuki Sugawara,*[a] Xiao Chen[b] Ryusei Higuchi[c] and Takeo Yamaguchi*[a]

[a]*Laboratory for Chemistry and Life Science, Institute of Innovative Research, Tokyo Institute of Technology, Nagatsuta 4259, Midori, Yokohama 226-8503, Japan.*

[b]*School of Engineering, Tokyo Institute of Technology, 4259 Nagatsuta, Midori, Yokohama, Kanagawa 226-8503, Japan*

[c]*Laboratory for Materials and Structures, Institute of Innovative Research, Tokyo Institute of Technology, 4259 Nagatsuta, Midori, Yokohama, 226-8503 Japan*

Correspondence to Yuuki Sugawara (E-mail: sugawara.y.aa@m.titech.ac.jp); Takeo Yamaguchi (E-mail: yamag@res.titech.ac.jp)

Methods

Machine learning programs and software

Machine learning (ML) models for prediction and analysis were constructed using the scikit-learn library 0.23.2 in Python 3.7.4.[1] Shapley additive explanations (SHAP) value for each feature was estimated using the SHAP library 0.40.0.[2] These machine learning processes were implemented using Spyder software 4.1.5.[3]

Data collection and structural features

To prepare the dataset for ML, data on the crystal structures and OER activities of 154 types of multimetal oxides were manually collected from 47 published articles. Table S1 presents a comprehensive list of the collected multimetal oxides and their respective data source. The following structural parameters were considered as explanatory variables: A–A distance (interatomic distance between two A-site metals), A–B distance, A–O distance, B–B distance, B–O distance, A–O–A angle (bond angle formed by neighbor A–O and O–A bonds), A–O–B angle, B–O–B angle, A polyhedral volume (polyhedral volume of A-site metal center and coordinated O atoms), B polyhedral volume, A effective coordination (effective coordination number of O atoms around A-site metal center), B effective coordination, A distortion index (index of distortion of the polyhedron with A-site metal center and coordinated O atoms), B distortion index and A ion radius. The effective coordination number and distortion index are defined by the following equations:

$$\text{effective coordination number} = \sum_i w_i \qquad (1)$$

$$w_i = \exp\left[1 - \left(\frac{d_i}{d_{av}}\right)^{Ca}\right] \quad (2)$$

$$\text{distortion index} = \frac{1}{\mathrm{n}}\sum_{i=1}^{\mathrm{n}} \frac{|d_i - d_{av}|}{d_{av}} \quad (3)$$

where d_i is the bond length from the central metal atom (M) to the ith coordinating O atom in the MO_x polyhedra, d_{av} is the weighted average M–O bond length and C_a is the apparent coordination number.

The parameters were collected based on the presented crystal structures in the published articles and extracted from the CIF files in ICSD or JCPDS using VESTA software.[4] For the dataset, maximum and minimum values of the structural parameter were employed instead of its average value because average values do not reflect the distributions of each parameter.

The OER activities were used as objective variables. To ensure comparability of OER activity between different data sources, the OER overpotentials were extracted from the onset potentials at a current density of 20–500 μA per surface area of oxide particles (cm^2_{oxide}) or 1–10 mA per electrode area (cm^2_{geo}), depending on the graphs presented in each paper. Since the polarized currents under OER are significantly changeable due to their catalyst loading amounts and specific surface areas,[5] the onset potential was used to define the overpotential. Finally, a dataset comprising 154 samples was obtained, consisting of four types of A-site (Ca, Sr, Ba and La) and twelve types of B-site metals (Ti, Cr, Mn, Fe, Co, Ni, Cu, Mo, Nb, Ru, Bi and Si).

Visualization of the data distribution

For the t-distributed stochastic neighbor embedding (t-SNE)[6] analysis, the hyperparameter perplexity was optimized and selected within the range of 5 and 105 based on the minimization of its k-nearest neighbor normalized error for visualization and reconstruction.[7]

ML models to identify importance of structural descriptors

The relative importance of structural descriptors for OER activity was examined using eight types of commonly used ML algorithms: multiple linear regression (MLR), least absolute shrinkage and selection operator regression (LASSO),[8] ridge regression (Ridge),[9] partial least-squares regression (PLS),[10] support vector regression (SVR),[11] random forest regression (RFR),[12] gradient boosted regression (GBR)[13] and extra trees regression (ETR).[14] The hyperparameters for each algorithm were optimized using the grid-search method, as shown in Table S2. The collected dataset was fitted using these eight ML algorithms, and the prediction accuracies were evaluated through cross-validation with 75 % and 25 % samples as training and test sets, respectively. The root-mean-squared error (RMSE) was used to compare the averaged error of the predicted OER overpotentials for each ML algorithm. The contribution of each explanatory variable to OER activity was quantified and ranked based on SHAP values.

Supplementary Tables and Figure

Table S1 List of 154 multimetal oxides collected as OER electrocatalysts from previously reported literature.

Literature	Chemical formula	Ref.
2011, Shao-Horn et al.	$LaCrO_3$ $LaMnO_{3+\delta}$ $LaMnO_3$ $LaMn_{0.5}Cu_{0.5}O_3$ $La_{0.5}Ca_{0.5}MnO_3$ $LaCoO_3$ $LaNiO_3$ $Ba_{0.5}Sr_{0.5}Co_{0.8}Fe_{0.2}O_{3-\delta}$ $La_{0.5}Ca_{0.5}CoO_{3-\delta}$ $LaMn_{0.5}Ni_{0.5}O_3$ $LaFeO_3$ $La_{0.75}Ca_{0.25}FeO_3$ $La_{0.5}Ca_{0.5}FeO_3$	15
2013, Shao-Horn et al.	$LaCoO_3$ $SrCo_{0.8}Fe_{0.2}O_{3-\delta}$ $Ba_{0.5}Sr_{0.5}Co_{0.8}Fe_{0.2}O_{3-\delta}$	16
2014, Zhang et al.	$LaNiO_3$	17
2015, Shao et al.	$Ba_{0.5}Sr_{0.5}Co_{0.8}Fe_{0.2}O_{3-\delta}$ $SrCo_{0.9}Ti_{0.1}O_{3-\delta}$ $SrFe_{0.9}Ti_{0.1}O_{3-\delta}$	18
2015, Shao et al.	$Ba_{0.5}Sr_{0.5}Co_{0.8}Fe_{0.2}O_{3-\delta}$ $SrCo_{0.8}Fe_{0.2}O_{3-\delta}$	19
2016, Liu et al.	$LaFeO_3$	20
2016, Stevenson et al.	$SrCoO_3$ $La_{0.2}Sr_{0.8}CoO_{3-\delta}$ $La_{0.4}Sr_{0.6}CoO_{3-\delta}$ $La_{0.6}Sr_{0.4}CoO_{3-\delta}$ $La_{0.8}Sr_{0.2}CoO_{3-\delta}$ $LaCoO_3$	21

2016, Lee et al.	$SrTiO_3$ $LaNiO_3$	22
2017, Luo et al.	$La_{0.8}Sr_{0.2}MnO_3$	23
2015, Schmidt et al.	$Ba_{0.5}Sr_{0.5}Co_{0.8}Fe_{0.2}O_{3-\delta}$	24
2017, Shao-Horn et al.	$LaCoO_3$ $SrCoO_3$	25
2018, Shao et al.	$La_{0.8}Sr_{0.2}FeO_{3-\delta}$ $LaFeO_{3-\delta}$	26
2018, Shao et al.	$SrFe_{0.85}Si_{0.15}O_{3-\delta}$ $SrFe_{0.9}Si_{0.1}O_{3-\delta}$	27
2018, Xu et al.	$LaFeO_3$	28
2017, Xu et al.	$LaCoO_3$ $LaCo_{0.9}Fe_{0.1}O_3$ $LaCo_{0.75}Fe_{0.25}O_3$ $LaCo_{0.5}Fe_{0.5}O_3$	29
2018, Yuan et al.	$SrNb_{0.1}Co_{0.7}Fe_{0.2}O_{3-\delta}$	30
2018, Shao-Horn et al.	$Sr_{0.5}Ca_{0.5}FeO_3$ $CaFeO_{3-\delta}$ $SrCoO_{3-\delta}$	31
2018, Yagi et al.	$CaVO_3$ $CaMnO_3$ $CaFeO_3$ $CaCoO_3$ $SrCrO_3$ $SrMnO_3$ $SrFeO_3$ $SrCoO_3$ $LaMnO_3$ $LaFeO_3$ $LaCoO_3$ $LaNiO_3$ $LaCuO_3$ $SrMn_{0.5}Fe_{0.5}O_3$ $Sr_{0.5}La_{0.5}FeO_3$ $CaMn_{0.5}Fe_{0.5}O_3$ $Ca_{0.5}La_{0.5}FeO_3$ $Sr_{0.5}La_{0.5}MnO_3$	32

	$LaMn_{0.5}Fe_{0.5}O_3$	
2019, Du et al.	$SrTiO_3$	33
2019, Gui et al.	$LaCoO_3$ $La_{0.9}Sr_{0.1}CoO_3$ $La_{0.7}Sr_{0.3}CoO_3$	34
2018, Grimaud et al.	$LaNiO_3$	35
2019, Yagi et al.	$SrRuO_3$ $Ca_{0.5}Sr_{0.5}RuO_3$ $CaRuO_3$	36
2013, Shao-Horn et al.	$Ba_6Mn_5O_{16}$ $CaMnO_3$ $LaMnO_{3+\delta}$ $La_{0.4}Sr_{0.6}CoO_3$ $LaCoO_3$	37
2014, Yang et al.	$CaMnO_3$	38
2015, Yagi et al.	$CaCu_3Fe_4O_{12}$ $Ba_{0.5}Sr_{0.5}Co_{0.8}Fe_{0.2}O_{3-\delta}$ $CaFeO_3$ $SrFeO_3$	39
2016, Smith	$SrCoO_3$	40
2017, Shao et al.	$Ba_2Bi_{0.1}Sc_{0.2}Co_{1.7}O_6$ $Ba_2Bi_{0.2}Sc_{0.2}Co_{1.6}O_6$ $Ba_{0.5}Sr_{0.5}Co_{0.8}Fe_{0.2}O_{3-\delta}$	41
2017, Tsuji et al.	$LaFe_{0.5}Co_{0.5}O_3$ $Ca_2Fe_2O_5$ $Ca_2Fe_{1.75}Co_{0.25}O_5$ $Ca_2Fe_{1.5}Co_{0.5}O_5$ $Ba_{0.5}Sr_{0.5}Co_{0.8}Fe_{0.2}O_{3-\delta}$ Ca_2FeCoO_5	42
2017, Luo et al.	$LaSr_3Fe_3O_{10}$ $LaSr_3Co_{1.5}Fe_{1.5}O_{10}$	43
2017, Yang et al.	$LaCoO_3$	44
2018, Yagi et al.	$CaCu_3Fe_4O_{12}$ $CaCu_3Ti_4O_{12}$ $CaCu_3Mn_4O_{12}$ $CaCu_3Co_4O_{12}$ $CaCu_3V_4O_{12}$	45

	$CaVO_3$ $CaMnO_3$ $CaFeO_3$ $CaCoO_3$ $LaCu_3Fe_4O_{12}$ $LaTi_{0.5}Cu_{0.5}O_3$ $LaCuO_3$ $LaFeO_3$ $LaMn_{0.5}Cu_{0.5}O_3$	
2017, Yagi et al.	$LaMnO_3$ $CaMnO_3$	46
2018, Shao et al.	$BaCoO_3$ Ba_2CoNbO_6 $Ba_2CoMo_{0.5}Nb_{0.5}O_6$	47
2018, Xie et al.	La_2NiMnO_6	48
2019, Habasaki et al.	Ca_2FeCoO_5 $Ca_2Fe_{1.5}Co_{0.5}O_5$ $Ca_2Fe_{1.75}Co_{0.25}O_5$	49
2019, Tavassol et al.	$CaSrFe_2O_6$ $Ca_2Fe_2O_6$	50
2019, Shao et al.	$Ba_2CoMo_{0.5}Nb_{0.5}O_6$ $BaCoO_3$	51
2019, Zhao et al.	$LaFeO_3$	52
2020, Shao-Horn et al.	$SrCoO_3$	53
2017, Jiang et al.	$LaCoO_3$	54
2019, Ramezanipur et al.	$CaSrFe_2O_6$ $Ca_2Fe_2O_6$	55
2020, Yamada et al.	$Sr_2FeMoO_{6-\delta}$ $LaFeO_3$ $Ca_2Fe_2O_5$ $CaFeO_3$ $LaCoO_3$ $Ca_2Co_2O_5$ $CaCoO_3$ $LaFe_{0.5}Co_{0.5}O_3$ Ca_2FeCoO_5 $Ba_{0.5}Sr_{0.5}Co_{0.8}Fe_{0.2}O_{3-\delta}$	56

	$CaCu_3Fe_4O_{12}$	
2020, Ramezanipor et al.	$SrMnO_{2.6}$ $SrMnO_3$	57
2020, Zeng et al.	$LaNiO_3$	58
2020, Okazaki et al.	$BaFe_2O_4$	59
2021, Yamaguchi et al.	$Ca_2Fe_2O_5$ $SrFeO_3$ $BaFeO_3$ $BaFe_2O_4$	60
2022, Yamaguchi et al.	$BaLaFeO_4$ $LaSrFeO_4$ $Sr_3Fe_2O_7$ $CaSrFe_2O_5$ $BaSrFe_4O_8$	61

Table S2 List of hyperparameters for ML algorithms.[a]

Category	Algorithm	Hyperparameters
Visualization	t-SNE	$5 \leq$ perplexity ≤ 105
Linear regression	MLR	–
	LASSO	$10^{-6} \leq \alpha \leq 10^{-2}$
	Ridge	$10^{-6} \leq \alpha \leq 10^{-2}$
	PLS	n_components ∈ [1, 2, 3, …, 28, 29, 30]
Nonlinear regression	SVR	kernel = rbf, C ∈ [2^{-5}, 2^{-4}, …, 2^{10}, 2^{11}], γ ∈ [2^{-20}, 2^{-19}, …, 2^{10}, 2^{11}], ε ∈ [2^{-10}, 2^{-9}, …, 2^{0}, 2^{1}],
	RFR	n_estimators ∈ [3, 5, 10], max_features ∈ [5, 10, 20, 30], min_samples_split ∈ [2, 5, 10], max_depth ∈ [5, 10, 50], min_samples_leaf ∈ [1, 2, 4]
	GBR	n_estimators ∈ [3, 5, 10], max_features ∈ [5, 10, , 20, 30], learning_rate ∈ [0.01, 0.1, 0.5], min_samples_split ∈ [2, 5, 10], max_depth ∈ [5, 10, 50], min_samples_leaf ∈ [1, 2, 4], subsample ∈ [0.2, 0.5, 1.0], min_weight_fraction_leaf ∈ [0.01, 0.1, 0.3, 0.5]
	ETR	n_estimators ∈ [3, 5, 10], max_features ∈ [5, 10, 20, 30], min_samples_split ∈ [2, 5, 10], max_depth ∈ [5, 10, 50], min_samples_leaf ∈ [1, 2, 4], min_weight_fraction_leaf ∈ [0.01, 0.1, 0.3, 0.5]

[a]The default values in each library were used for other nonmentioned hyperparameters.

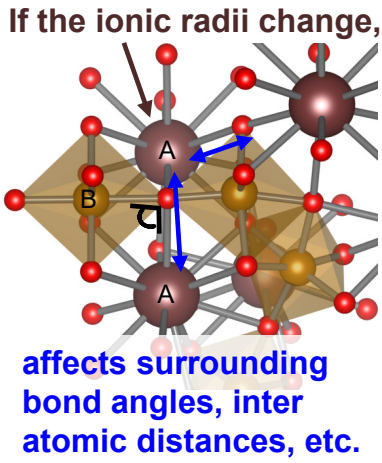

Fig. S1 Schematic illustration of the effect of A-site ionic radii on other structural parameters.

References

1 F. Pedregosa, G. Varoquaux, A. Gramfort, V. Michel, B. Thirion, O. Grisel, M. Blondel, P. Prettenhofer, R. Weiss, V. Dubourg, J. Vanderplas, A. Passos, D. Cournapeau, M. Brucher, M. Perrot and E. Duchesnay, *J. Mach. Learn. Res.*, 2011, **12**, 2825–2830.

2 S. M. Lundberg and S. I. Lee, *A Unified Approach to Interpreting Model Predictions*, 31st Annual Conference on Neural Information Processing Systems (NIPS), Long Beach, CA, 2017.

3 A. Kadiyala and A. Kumar, *Environ. Prog. Sustain. Energy*, 2017, **36**, 1580–1586.

4 K. Momma and F. Izumi, *J. Appl. Crystallogr.*, 2011, **44**, 1272–1276.

5 S. N. Sun, H. Y. Li and Z. C. J. Xu, *Joule*, 2018, **2**, 1024–1027.

6 L. van der Maaten, *J. Mach. Learn. Res.*, 2014, **15**, 3221–3245.

7 H. Kaneko, *Chemometrics Intell. Lab. Syst.*, 2018, **176**, 22–33.

8 R. Tibshirani, *J. R. Stat. Soc. Ser. B-Methodol.*, 1996, **58**, 267–288.

9 A. E. Hoerl and R. W. Kennard, *Technometrics*, 1970, **12**, 55–67.

10 S. Wold, M. Sjostrom and L. Eriksson, *Chemometrics Intell. Lab. Syst.*, 2001, **58**, 109–130.

11 H. Drucker, C. J. C. Burges, L. Kaufman, A. Smola and V. Vapnik, Denver, Co, 1996.

12 L. Breiman, *Mach. Learn.*, 2001, **45**, 5–32.

13 J. H. Friedman, *Ann. Stat.*, 2001, **29**, 1189–1232.

14 P. Geurts, D. Ernst and L. Wehenkel, *Mach. Learn.*, 2006, **63**, 3–42.

15 J. Suntivich, K. J. May, H. A. Gasteiger, J. B. Goodenough and Y. Shao-Horn, *Science*, 2011, **334**, 1383–1385.

16 M. Risch, A. Grimaud, K. J. May, K. A. Stoerzinger, T. J. Chen, A. N. Mansour and Y. Shao-Horn, *J. Phys. Chem. C*, 2013, **117**, 8628–8635.

17 Z. Z. Du, P. Yang, L. Wang, Y. H. Lu, J. B. Goodenough, J. Zhang and D. W. Zhang, *J. Power Sources*, 2014, **265**, 91–96.

18 C. Su, W. Wang, Y. B. Chen, G. M. Yang, X. M. Xu, M. O. Tade and Z. P. Shao, *ACS Appl. Mater. Interfaces*, 2015, **7**, 17663–17670.

19 Y. L. Zhu, W. Zhou, Z. G. Chen, Y. B. Chen, C. Su, M. O. Tade and Z. P. Shao, *Angew. Chem. Int. Ed.*, 2015, **54**, 3897–3901.

20 Y. L. Zhu, W. Zhou, J. Yu, Y. B. Chen, M. L. Liu and Z. P. Shao, *Chem. Mater.*, 2016, **28**, 1691–1697.

21 J. T. Mefford, X. Rong, A. M. Abakumov, W. G. Hardin, S. Dai, A. M. Kolpak, K. P. Johnston and K. J. Stevenson, *Nat. Commun.*, 2016, **7**, 11053.

22 J. R. Petrie, V. R. Cooper, J. W. Freeland, T. L. Meyer, Z. Y. Zhang, D. A. Lutterman and H. N. Lee, *J. Am. Chem. Soc.*, 2016, **138**, 2488–2491.

23 L. T. Yan, Y. Lin, X. Yu, W. C. Xu, T. Salas, H. Smallidge, M. Zhou and H. M. Luo, *ACS Appl. Mater. Interfaces*, 2017, **9**, 23820–23827.

24 E. Fabbri, M. Nachtegaal, X. Cheng and T. J. Schmidt, *Adv. Energy Mater.*, 2015, **5**, 1402033.

25 A. Grimaud, O. Diaz-Morales, B. H. Han, W. T. Hong, Y. L. Lee, L. Giordano, K. A. Stoerzinger, M. T. M. Koper and Y. Shao-Horn, *Nat. Chem.*, 2017, **9**, 457–465.

26 S. X. She, J. Yu, W. Q. Tang, Y. L. Zhu, Y. B. Chen, J. Sunarso, W. Zhou and Z. P. Shao, *ACS Appl. Mater. Interfaces*, 2018, **10**, 11715–11721.

27 X. M. Xu, Y. B. Chen, W. Zhou, Y. J. Zhong, D. Q. Guan and Z. P. Shao, *Adv. Mater. Interfaces*, 2018, **5**, 1701693.

28 H. Y. Li, Y. B. Chen, S. B. Xi, J. X. Wang, S. N. Sun, Y. M. Sun, Y. H. Du and Z. C. J. Xu, *Chem. Mater.*, 2018, **30**, 4313–4320.

29 Y. Duan, S. N. Sun, S. B. Xi, X. Ren, Y. Zhou, G. L. Zhang, H. T. Yang, Y. H. Du and Z. C. J. Xu, *Chem. Mater.*, 2017, **29**, 10534–10541.

30 H. Liu, X. F. Ding, L. X. Wang, D. Ding, S. H. Zhang and G. L. Yuan, *Electrochim. Acta*, 2018, **259**, 1004–1010.

31 B. H. Han, A. Grimaud, L. Giordano, W. T. Hong, O. Diaz-Morales, L. Yueh-Lin, J. Hwang, N. Charles, K. A. Stoerzinger, W. L. Yang, M. T. M. Koper and Y. Shao-Horn, *J. Phys. Chem. C*, 2018, **122**, 8445–8454.

32 I. Yamada, A. Takamatsu, K. Asai, T. Shirakawa, H. Ohzuku, A. Seno, T. Uchimura, H. Fujii, S. Kawaguchi, K. Wada, H. Ikeno and S. Yagi, *J. Phys. Chem. C*, 2018, **122**, 27885–27892.

33 L. Wang, K. A. Stoerzinger, L. Chang, X. M. Yin, Y. Y. Li, C. S. Tang, E. D. Jia, M. E. Bowden, Z. Z. Yang, A. Abdelsamie, L. You, R. Guo, J. S. Chen, A. Rusydi, J. L. Wang, S. A. Chambers and Y. G. Du, *ACS Appl. Mater. Interfaces*, 2019, **11**, 12941–12947.

34 Y. Lu, A. J. Ma, Y. F. Yu, R. Tan, C. W. Liu, P. Zhang, D. Liu and J. Z. Gui, *ACS Sustainable Chem. Eng.*, 2019, **7**, 2906–2910.

35 C. Z. Yang, M. Batuk, Q. Jacquet, G. Rousse, W. Yin, L. T. Zhang, J. Hadermann, A. M. Abakumov, G. Cibin, A. Chadwick, J. M. Tarascon and A. Grimaud, *ACS Energy Lett.*, 2018, **3**, 2884–2890.

36 S. Hirai, T. Ohno, R. Uemura, T. Maruyama, M. Furunaka, R. Fukunaga, W. T. Chen, H. Suzuki, T. Matsuda and S. Yagi, *J. Mater. Chem. A*, 2019, **7**, 15387-15394.

37 A. Grimaud, C. E. Carlton, M. Risch, W. T. Hong, K. J. May and Y. Shao-Horn, *J. Phys. Chem. C*, 2013, **117**, 25926–25932.

38 J. Kim, X. Yin, K. C. Tsao, S. H. Fang and H. Yang, *J. Am. Chem. Soc.*, 2014, **136**, 14646–14649.

39 S. Yagi, I. Yamada, H. Tsukasaki, A. Seno, M. Murakami, H. Fujii, H. Chen, N. Umezawa, H. Abe, N. Nishiyama and S. Mori, *Nat. Commun.*, 2015, **6**, 8249.

40 H. A. Tahini, X. Tan, U. Schwingenschlogl and S. C. Smith, *ACS Catal.*, 2016, **6**, 5565–5570.

41 H. N. Sun, G. Chen, Y. L. Zhu, B. Liu, W. Zhou and Z. P. Shao, *Chem. Eur. J.*, 2017, **23**, 5722–5728.

42 E. Tsuji, T. Motohashi, H. Noda, D. Kowalski, Y. Aoki, H. Tanida, J. Niikura, Y. Koyama, M. Mori, H. Arai, T. Ioroi, N. Fujiwara, Y. Uchimoto, Z. Ogumi and H. Habazaki, *ChemSusChem*, 2017, **10**, 2864–2868.

43 S. B. Liu, H. Luo, Y. H. Li, Q. X. Liu and J. L. Luo, *Nano Energy*, 2017, **40**, 115–121.

44 J. Kim, X. X. Chen, P. C. Shih and H. Yang, *ACS Sustainable Chem. Eng.*, 2017, **5**, 10910–10917.

45 I. Yamada, A. Takamatsu, K. Asai, H. Ohzuku, T. Shirakawa, T. Uchimura, S. Kawaguchi, H. Tsukasaki, S. Mori, K. Wada, H. Ikeno and S. Yagi, *ACS Appl. Energy Mater.*, 2018, **1**, 3711–3721.

46 I. Yamada, H. Fujii, A. Takamatsu, H. Ikeno, K. Wada, H. Tsukasaki, S. Kawaguchi, S. Mori and S. Yagi, *Adv. Mater.*, 2017, **29**, 1603004.

47 H. N. Sun, G. Chen, J. Sunarso, J. Dai, W. Zhou and Z. P. Shao, *ACS Appl. Mater. Interfaces*, 2018, **10**, 16939–16942.

48 Y. Tong, J. C. Wu, P. Z. Chen, H. F. Liu, W. S. Chu, C. Z. Wu and Y. Xie, *J. Am. Chem. Soc.*, 2018, **140**, 11165–11169.

49 D. Kowalski, H. Kiuchi, T. Motohashi, Y. Aoki and H. Habazaki, *ACS Appl. Mater. Interfaces*, 2019, **11**, 28823–28829.

50 C. Bloed, J. Vuong, A. Enriquez, S. Raghavan, I. Tran, S. Derakhshan and H. Tavassol, *ACS Appl. Energy Mater.*, 2019, **2**, 6140–6145.

51 H. N. Sun, J. He, Z. W. Hu, C. T. Chen, W. Zhou and Z. P. Shao, *Electrochim. Acta*, 2019, **299**, 926–932.

52 J. Zhang, Y. X. Cui, L. C. Jia, B. B. He, K. Zhang and L. Zhao, *Int. J. Hydrog. Energy*, 2019, **44**, 24077–24085.

53 D. A. Kuznetsov, J. Y. Peng, L. Giordano, Y. Roman-Leshkov and Y. Shao-Horn, *J. Phys. Chem. C*, 2020, **124**, 6562–6570.

54 K. Liu, J. Li, Q. F. Wang, X. P. Wang, D. Qian, J. B. Jiang, J. H. Li and Z. H. Chen, *J. Alloy. Compd.*, 2017, **725**, 260–269.

55 R. K. Hona and F. Ramezanipour, *Angew. Chem. Int. Ed.*, 2019, **58**, 2060–2063.

56 I. Yamada, M. Kinoshita, S. Oda, H. Tsukasaki, S. Kawaguchi, K. Oka, S. Mori, H. Ikeno and S. Yagi, *Chem. Mater.*, 2020, **32**, 3893–3903.

57 R. K. Hona and F. Ramezanipour, *Inorg. Chem.*, 2020, **59**, 4685–4692.

58 C. Cao, C. Y. Shang, X. Li, Y. Y. Wang, C. X. Liu, X. Y. Wang, S. M. Zhou and J. Zeng, *Nano Lett.*, 2020, **20**, 2837–2842.

59 Y. Okazaki, I. Yamada and S. Yagi, *Mater. Trans.*, 2020, **61**, 1523–1526.

60 Y. Sugawara, K. Kamata, A. Ishikawa, Y. Tateyama and T. Yamaguchi, *ACS Appl. Energy Mater.*, 2021, **4**, 3057–3066.

61 Y. Sugawara, S. Ueno, K. Kamata and T. Yamaguchi, *ChemElectroChem*, 2022, **9**, e202101679.